Order-Disorder Events Produced by Single Vacancy Migration*

J. R. BEELER, JR., AND J. A. DELANEY
General Electric Company, Nuclear Materials and Propulsion Operation, Cincinati, Ohio
(Received 20 December 1962)

Monte Carlo computational experiments, based on the Flinn-McManus method, were used to study the interaction between ordering (disordering) and single vacancy migration in AB alloys. Square planar, simple cubic, and bcc lattices were studied. If the alloy is initially disordered (short-range order near zero), the extent of vacancy migration for N jumps is slightly larger than that for a symmetric random walk. However, when the initial short-range order is either comparable to or larger than the equilibrium value for the critical temperature, the ordering process contracts the extent of vacancy migration relative to that for a symmetric random walk. In two dimensions (surface diffusion) the degree of contraction depends upon the number of jumps and is larger than that for three dimensions (bulk diffusion) which is independent of the number of jumps. The long- and short-range order established in expanding migration regions by 10^4 to 3×10^4 vacancy jumps are very close to the values predicted by Bethe's model for the equilibrium state. A system of contiguous antiphase domains was formed in an initially disordered alloy, by single vacancy migration, rather than a single ordered nucleus.

1. INTRODUCTION

THIS paper concerns computational experiments on the interaction between ordering (disordering) and single vacancy migration in an AB alloy, at the beginning of the ordering (disordering) process. The Monte Carlo method of Flinn and McManus[1] was used to describe, approximately, the microscopic detail of vacancy migration for lifetimes of the order of 3×10^4 jumps in a square planar lattice (SPL) and 10^4 jumps in a simple cubic lattice (SCL). The description includes: (1) the structure of the vacancy migration path, (2) the spatial extent of vacancy migration as a function of the number of jumps, (3) a mapping of the atomic order pattern during migration, i.e., the evolution of antiphase domains during either ordering or disordering, and (4) the change in configurational energy as a function of the number of jumps.

A microscopic description of vacancy migration is of interest both from the standpoint of diffusion theory, per se, and those aspects of defect annealing connected with diffusion. Atomic diffusion in orderable alloys is influenced by their ordering energy. This effect has been observed, for example, by Kuper *et al.*[2] for the diffusion of Cu^{64}, Zn^{65}, and Sb^{124} in β-brass. The atomic diffusion coefficients were found to be significantly smaller when the host material was in a highly ordered state than when it was disordered and the diffusion coefficient could not be described by the usual Arrhenius equation. Small effects due to short-range order were observed in the disordered state. In this regard we centered our interest on a comparison of the number of different atomic sites, Σ, visited by the vacancy in N jumps in an orderable system with that for a symmetric random walk, i.e., zero ordering energy. A comparison of the mean square displacement and a linear displacement metric for these two cases was also made. A recent article by Rudman[3] on inhomogeneous ordering in the neighborhood of dislocations indicates an additional area wherein the microscopic behavior of vacancy migration in alloys is of interest.

In pure metals, a vacancy lifetime is of the order of 10^8–10^{10} jumps. Recently, Wechsler and Kernohan[4] and Tucker and Webb[5] have suggested that a shorter lifetime of the order of 10^4–10^5 jumps may be appropriate for the excess vacancies in quenched alloys. If this is correct, our results are immediately applicable to quenched material. However, even if realistic lifetimes are considerably larger than the $\sim10^4$ jump lifetimes treated in our calculations, the results are still applicable to these longer lifetimes provided the individual migration regions associated with each vacancy do not overlap. This, we feel, is the essential restriction on the applicability of our results. For example, the calculations indicate that for a vacancy concentration of 10^{-5} vacancy per atom, the migration regions of individual, uniformly distributed vacancies would begin to interact after about 10^5 jumps in the SCL and after about 10^6 jumps in the SPL in an initially disordered system. The planar lattice calculations apply, qualitatively, to very thin films and perhaps surface diffusion. Because it is relatively easy to visualize the two-dimensional results, we have found them helpful in interpreting the results of our current three-dimensional studies for simple cubic, bcc, and fcc lattices.

2. COMPUTATIONAL MODEL

The Monte Carlo model of Flinn and McManus[1] was used in this study. Some calculations were also performed using the model of Metropolis *et al.*,[6] but these

* Work supported by the U. S. Atomic Energy Commission Contract No. AT(40-1)-2847 and the U. S. Air Force, Aeronautical Systems Division, Air Force Systems Command, Contract No. AF 33(657)-8473.

[1] P. A. Flinn and G. M. McManus, Phys. Rev. **124**, 54 (1961).

[2] A. B. Kuper, D. Lazarus, J. R. Manning, and C. T. Tomizuka, Phys. Rev. **104**, 1536 (1956).

[3] P. S. Rudman, Acta Met. **10**, 195 (1962).

[4] M. S. Wechsler and R. H. Kernohan, Acta Met. **7**, 599 (1959).

[5] C. W. Tucker and M. B. Webb, Acta Met. **7**, 187 (1959).

[6] N. Metropolis, A. W. Rosenbluth, M. N. Rosenbluth, A. H. Teller, and E. Teller, J. Chem. Phys. **21**, 1087 (1953).

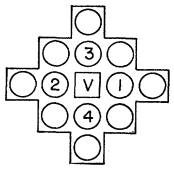

FIG. 1. Jump cell for the square planar lattice. V (position 0) denotes the vacancy position before a jump. The numbered sites are the four possible terminal positions for a vacancy jump. In general, a knowledge of the occupancy of all sites in the jump cell is required in order to select a vacancy jump direction.

results are not reported. The Flinn-McManus model was specifically designed to approximate the kinetics of single vacancy movement in orderable systems. The Metropolis model was designed to compute equilibrium configurations without specification of a particular mechanism for the approach to equilibrium. These two models give different results, but the difference is not as great as one might expect.

The configurational energy of any subset of the lattice was assumed to be the number of "unlike bonds" it contained multiplied by $-v$, the energy per unlike bond. (The energy v is called the ordering energy.[7-9]) In a binary crystal of A and B atoms an $A-B$ bond is an unlike bond. The energy of like bonds, e.g., $A-A$ and $B-B$ bonds, was taken to be zero. The justification for this procedure is explained, for example, by Nix and Shockley.[7] In the Flinn-McManus model, a particular vacancy jump direction is determined by a two-part rejection technique.[10] First of all, an atom on one of the z first neighbor sites of the vacancy is selected at random (see Fig. 1). Call this site the ith site and the vacancy position the zeroth site. The transition probability p_{0i} of Eq. (1) is then used to determine if the atom on

$$p_{0i}=e^{\Delta n_{0i}\phi}/(1+e^{\Delta n_{0i}\phi}), \tag{1}$$

the ith site and the vacancy are to interchange positions. This is the second part of the sampling technique. Δn is the number of unlike bonds that would be *gained* if the interchange were to occur and $\phi\equiv v/kT$. This rejection technique is repeated until a jump occurs.

In the Metropolis rejection technique, the transition probability p_{0i}^* of Eq. (2) is used if Δn_{0i} is negative, and $p_{0i}^*=1$ if $\Delta n_{0i}\geq 0$.

$$p_{0i}^*=e^{\Delta n_{0i}\phi} \quad (\Delta n_{0i}<0). \tag{2}$$

Both models satisfy the three conditions which a transition probability definition must meet.[11] In short, these conditions are (a) the normalization condition, (b) the ergodic condition, and (c) the condition of microscopic reversibility. It is perhaps worthwhile to compare these two rejection techniques. The Flinn-McManus model gives $p_{0i}=\frac{1}{2}$ for $\Delta n_{0i}=0$ while the Metropolis definition gives $p_{0i}^*=1$. Further, the Flinn-McManus model assigns *different* p_{0i} values to trials with different $\Delta n_{0i}>0$, whereas $p_{0i}^*=1$ whenever $\Delta n_{0i}>0$ in the Metropolis model. Forcing a jump, so to speak, whenever $\Delta n_{0i}\geq 0$, is appropriate when a description of the kinetic aspects of an approach to equilibrium is not wanted. A distinction between the probabilities for transition to states of different lower energies is necessary in a kinetic approximation, such as that developed by Flinn and McManus.

Physically, the computational experiments described here correspond to watching vacancy movement in a specimen subsequent to a sudden temperature change. The specimen is assumed to have an initial equilibrium long-range order (LRO) S_i associated with an initial temperature T_i. The temperature is then suddenly changed to a different value T_f and the migratory behavior of a single vacancy is followed as it participates in the establishment of the equilibrium LRO for temperature T_f. There will also be participation by divacancies but this effect is ignored. The original site occupancy pattern at T_i was selected by assigning right occupancy with probability p_r given by Eq. (3) at any given site

$$p_r=(S_i+1)/2. \tag{3}$$

This sampling procedure is a zeroth order approximation to reality in that it ignores the nonrandom arrangement of atoms due to short-range order (SRO).[12] In the case of the SPL, the use of this occupancy sampling method imposes a severe restriction on the choice of initial states because it fails to give a good approximation to the correct SRO unless the alloy initially is either completely ordered or completely disordered. In the case of the SCL, however, the sampled SRO is, for our purposes, sufficiently close to the true SRO if $S_i\geq 0.8$. In effect, the occupancy pattern for an infinite lattice was first determined using Eq. (3). The initial vacancy site was then selected at random and the particulars of each vacancy jump recorded. In practice the occupancy specifications were done in an equivalent but considerably different manner to conserve memory storage space on the computer (32 000 words in the IBM 7090 computer). The initial vacancy position was always taken to be $\mathbf{r}=0$. After the first ith trial site in the two-part sampling scheme had been selected, the occupancies of ith site and vacancy site first neighbors were selected and the associated transition probability computed. In general, whenever the vacancy moved, first-neighbor sites of unknown occupancy would appear about a trial site. In these instances the computer assigned right (R) or wrong (W) occupancy according to Eq. (3) before proceeding with the calculation. Both the original occupancy pattern and the current occupancy pattern were retained in the computer memory, the latter being used in the transition probability calculations. Each

[7] F. C. Nix and W. Shockley, Rev. Mod. Phys. **10**, 1 (1938).
[8] T. Muto and Y. Takagi, in *Solid State Physics*, edited by F. Seitz and D. Turnbull (Academic Press Inc., New York, 1955), Vol. 1, p. 194.
[9] L. Guttman, in *Solid State Physics*, edited by F. Seitz and D. Turnbull (Academic Press Inc., New York, 1956), Vol. 3, p. 145.
[10] H. Kahn, U. S. Atomic Energy Commission Report AECU-3259, 1954 (unpublished), see pp. 10–15.
[11] W. W. Wood and F. R. Parker, J. Chem. Phys. **27**, 720 (1957).
[12] J. M. Cowley, Phys. Rev. **77**, 669 (1950).

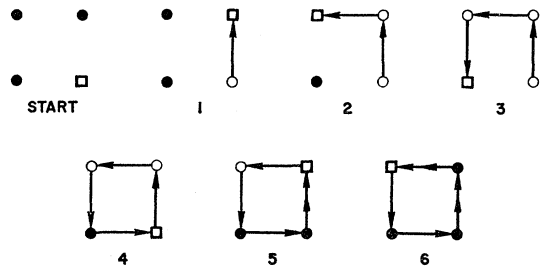

FIG. 2. Elcock six-jump cycle in a perfectly ordered alloy. Right and wrong occupancy are denoted by filled and open circles, respectively. The open square represents the vacancy.

memory location was packed to accommodate nine lattice sites. The lattice coordinate system was floated to minimize the number of unused memory locations.

For each assignment of ϕ, S_i, and N, ten different pseudorandom number sequences $G_1, \cdots, G_{10}$ were used to account in part for the distribution of short-range order associated with a given S_i. A single run was, therefore, specified by (ϕ,S_i,N,G_j). The averaged results for 10 runs comprised the results of an experiment.

3. MIGRATION IN AN INITIALLY PERFECTLY ORDERED ALLOY

Vacancy migration characteristics in a partially ordered alloy can be thought of as being a mixture of those manifest in a perfectly ordered system and those exhibited in a completely disordered system. Specifically, our results for the SPL indicate that vacancy migration behavior in a highly ordered local region of a partially ordered alloy is exactly that observed in a perfectly ordered alloy, as one would expect, and that the process of antiphase domain growth in a partially ordered alloy closely resembles the *coalescence* of antiphase domains in an initially disordered alloy. Because of these similarities, a somewhat detailed description of the basic jump sequences observed in perfectly ordered and disordered alloys is pertinent. The jump sequences observed in perfectly ordered alloys appear to be the most fundamental and will be discussed first.

Elcock[13] has shown that the most probable vacancy jump sequence, which simultaneously gives a net transport of atoms and the vacancy, and the preservation of order, is the six-jump cycle diagrammed in Fig. 2 wherein filled and open circles represent rightly occupied sites (R sites) and wrongly occupied sites (W sites), respectively. Elcock suggests that this six-jump cycle is the dominant transport mode provided $S\simeq 1.0$ and ϕ is about $2\phi_c$ or larger, where $\phi_c=v/kT_c$ and T_c is the critical temperature. Our results are in agreement with Elcock for $\phi\simeq 2\phi_c$ and, furthermore, indicate that this six-jump is important even for $\phi\simeq\phi_c$ in alloys with perfect initial order.

Several 500-jump histories were run for $\phi=1.5$ and $\phi=0.8$ in a perfectly ordered system. Because $\phi_c\simeq 0.7$ in a square planar lattice, our results for $\phi=1.5$ can be compared with Elcock's ideas. Three types of jump sequences were observed which led to a net transport of atoms and the vacancy with preservation of order for $\phi=1.5$. One of these was the Elcock loop, the second an inefficiently negotiated Elcock loop with retracted spurs and the third was a 10-jump double loop. Figure 3 illustrates the types of inefficient Elcock loops observed. The numbers at the right of a lattice site denote the jump number for which that site was the terminal position. In (a) the loop is interrupted by a single external spur excursion, in (b) by an external L-shaped spur excursion, and in (c) both by an external spur excursion and retracing along one side of the loop itself. In each case the effective path is an Elcock loop, and no more than three W sites appear at any given time. The 10-jump double loop is described by Fig. 4. In the double loop no more than five W sites occur at any given time. This double loop was the most complicated order preserving transport path observed for $\phi=1.5$. Six 500-jump histories were examined in detail. Double loops occurred about one-half as frequently as Elcock loops and inefficient Elcock loops about 3.5 times as frequently as Elcock loops. The probability for an Elcock loop appearing in six consecutive jumps is 2.5×10^{-3} for $\phi=1.5$ and $S_i=1$.

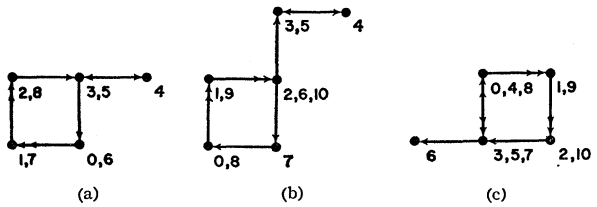

FIG. 3. Inefficient Elcock loops observed for $S_i=1$ and $\phi=1.5$.

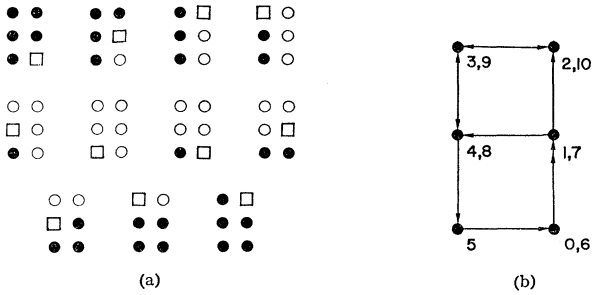

FIG. 4. Double loop observed for $S_i=1$ and $\phi=1.5$.

At least 90% of the vacancy jumps were consumed in retracted excursions emanating from sites which were the terminal positions for jumps in the effective order preserving sequences described above. Linear excursions with a maximum length of three lattice spacings were the most frequently occurring retracted excursions. Figure 5 describes a typical areal excursion which the vacancy tends to make when it "fails" to complete a

[13] E. W. Elcock, Proc. Phys. Soc. (London) 73, 250 (1959).

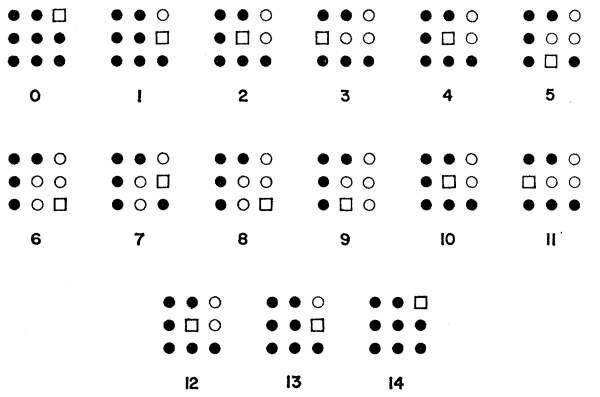

FIG. 5. Retracted areal excursion observed for $S_i=1$ and $\phi=1.5$.

possible inefficient loop. Note that after jumps (2), (4), (10), and (12) the vacancy was in position to execute the fourth leg of an Elcock loop.

The 30 000-jump history runs gave the change in configurational energy every 100 jumps. On the basis of these data, it appears as if about 0.04 AB bonds were broken per 1000 jumps in the wake of the vacancy migration path when $S=1.0$ and $\phi=1.5$. About 250 broken AB bonds are produced per 1000 jumps when $\phi=0$.

When ϕ is reduced to 0.8, rather than immediately removing the wrongly occupied sites left in the wake of an "unsuccessful" attempt toward an order preserving transport path, as it does when $\phi=1.5$, the vacancy tends continually to produce more wrongly occupied sites. A small fraction of these sites escape re-ordering attempts and the alloy gradually becomes disordered. However, most of wrongly occupied sites are removed by being collected into an antiphase domain which is then systematically removed in such a way as to restore perfect order, locally, and also contribute to a net transport of atoms and the vacancy. This antiphase domain is removed either by an inwardly spiraling path along its periphery or by linear traverses along successive rows or columns. This type of behavior requires a relatively large number of jumps, and the effect of any given jump has an even chance of being negated by that of a subsequent jump.

TABLE I. Effective path for antiphase domain formation and row-by-row removal observed for $S_i=1.0$ and $\phi=0.8$.

Jump number	Jump direction	Energy change	Cumulative energy change	
1	3	−3	−3	
2	3	−2	−5	
3	1	−2	−7	First
4	4	−1	−8	stage
5	2	0	−8	
6	3	+1	−7	
7	1	+3	−4	
8	4	+3	−7	
9	4	−1	−8	
10	4	−1	−9	
11	2	−1	−10	
12	2	−1	−11	
13	3	−1	−12	
14	3	−1	−13	Second
15	1	0	−13	stage
16	3	+1	−12	
17	1	+1	−11	
18	3	−2	−13	
19	2	−2	−15	
20	4	0	−15	
21	2	+1	−14	
22	4	0	−14	
23	1	−1	−15	
24	3	−1	−16	
25	3	+1	−15	Third
26	1	+2	−13	stage
27	4	+2	−11	
28	4	+2	−9	
29	4	+1	−8	
30	2	0	−8	
31	2	+1	−7	Fourth
32	4	+2	−5	stage
33	1	+2	−3	
34	1	+3	0	

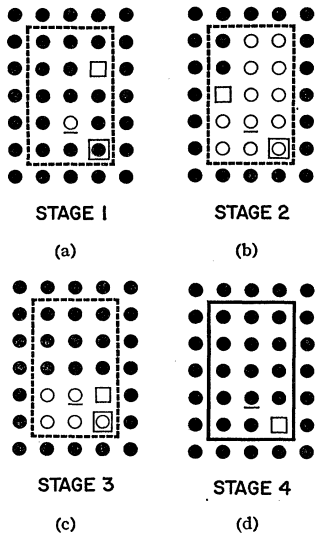

FIG. 6. Construction and removal of a small antiphase region observed for $S_i=1$ and $\phi=0.8$.

Net transport by pure and inefficient Elcock loops as well as by inefficient double loops was observed for $\phi=0.8$. Pure loops occurred more frequently than when $\phi=1.5$ (the probability for an Elcock loop in six consecutive jumps is 6.7×10^{-3} for $\phi=0.8$, and 2.5×10^{-3} for $\phi=1.5$). The major difference between migration for $\phi=0.8$ and that for $\phi=1.5$ was the appearance of net transport and order preserving paths entailing 100–200 jumps and involving blocks of 20–30 sites. Because a similar type of transport is important in partially ordered alloys, but is there complicated by a partially disordered environment, an example of two related but more simple types of antiphase domain removal observed in the $S_i=1$, $\phi=0.8$ experiments will be discussed.

The path concerned required a total 154 jumps of which 34 were effective jumps (22%). Table I lists the effective jump number, the jump direction, and the

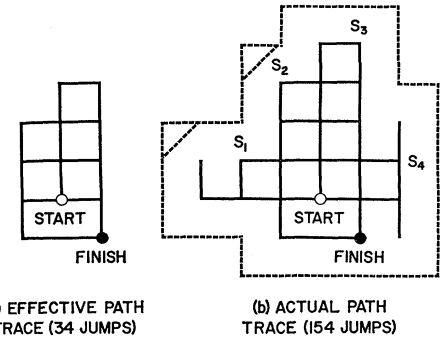

FIG. 7. Effective path trace (a) and actual path trace (b) followed by the vacancy in constructing and removing the antiphase region of Fig. 6.

configurational energy change in terms of AB bonds gained. The numbers 3 and 4 indicate a vacancy jump upward and downward, respectively, while 1 and 2 signify a rightward and leftward jump (see Fig. 1). It is convenient to divide the path into four stages. The first stage consists of jumps 1–7, jumps 2–7 comprising an Elcock loop (the energy changes in this loop are slightly different than those for a normal loop because of the wrong site positioned at the lower left corner of the loop). At the end of the first stage the occupancy pattern was that shown in Fig. 6(a). As before, R sites and W sites are designated by filled circles and open circles, respectively. The underscored site is the initial vacancy position. This site is wrongly occupied and is positioned just outside the jump cell for the immediately ensuing jump (jump 8). Stage two consists of jumps 8–22 of the effective path. Figure 6(b) shows that the occupancy pattern contained $12W$ sites at the end of the second stage. Jumps 23–29 of the third stage change the occupancy pattern to that of Fig. 6(c). In stage four, the vacancy moved to the left along the upper row of W sites in Fig. 6(c), down one jump and then to the right along the bottom row of W sites to terminate the transport path at the boxed site denoted by the circle in the square.

In other instances, the type of configuration shown in Fig. 6(b) was also removed by the vacancy either moving upward or downward along the left-most column to create a rectangular area of W sites. These jumps involve no energy change. In either case the vacancy can then follow the periphery of the antiphase region in a sequence of zero-energy change jumps. At each corner it will cause a gain of one AB bond. When the antiphase domain was large, a mixture of inward spiral, row-deletion and column-deletion paths were observed.

The antiphase domain formation and removal path described above represents the type of jump sequence used by the vacancy to remove an *isolated* W site. An isolated W site is one positioned outside the jump cell centered on the vacancy in an otherwise perfectly ordered region. If, as in this example, the isolated site is close enough to the vacancy that it can be included in the jump cell after a jump in at least one of the four possible jump directions, the vacancy will usually adopt the antiphase domain formation and removal technique. If, however, the isolated site is sufficiently far from the vacancy that two or more effective jumps in its direction are required to place it in the jump cell, the isolated site will tend to remain permanently and contribute to disordering. Isolated W sites are formed by paths similar to the first stage of the effective path defined by Table I. In conclusion, it appears that the most probable transport jump sequence of $\phi \geq \phi_c$ is one with an Elcock loop as its effective path. If the vacancy gets out of this loop, the most probable recovery path is one which temporarily disorders a large rectangular region and then removes this region by some combination of row, column, and peripheral deletion of W sites.

The effective path trace and the actual path trace for the antiphase formation and removal process defined by Table I are shown in Fig. 7. The spurs s_1-s_4 in the actual path trace of 154 jumps were of no consequence because the perfectly ordered environment was infinite. If, for example, the environment had contained W sites within the range of spurs s_1-s_4, the antiphase formation and removal process would have been more complicated. Suppose, for a moment, that the jump sequence had taken place in a locally ordered region contained in a partially ordered alloy. Because spur s_1 penetrated two lattice constants into the environment and spurs s_2, s_3, and s_4 one lattice constant beyond the effective path, the ordered region would have had to be at least as large as that defined by the dashed outline to contain the vacancy. A W site anywhere on this boundary could interrupt the antiphase formation and removal process. The removal of isolated wrongly occupied (rightly occupied) sites in partially ordered alloys begins just as it does in a perfectly ordered alloy

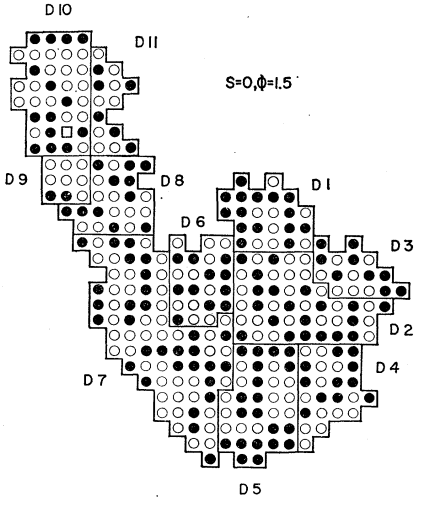

FIG. 8. Initial occupancy pattern of the 500-jump migration region.

but is rarely carried to completion because of interruptions caused by engagements with "extraneous" wrongly occupied (rightly occupied) sites in the immediate environment. As a consequence of these interruptions, antiphase domains in partially ordered alloys are usually formed by several passes of the vacancy path through the region they eventually occupy. In this context, the distribution of strings of sites of different occupancy than their first neighbors becomes important. We call such strings "minority strings" and discuss their function in the following subsection on vacancy migration in initially disordered alloys.

4. MIGRATION IN AN INITIALLY DISORDERED ALLOY

In agreement with experimental findings, antiphase domains were produced during the first stage of vacancy migration in an initially disordered alloy, i.e., $S_i=\sigma_i=0$. These domains were formed in a relatively small number of jumps provided ϕ was large, i.e., $\phi\sim1.5$. A somewhat detailed example of domain formation during the first 500 jumps of a 30 000-jump history will be given for $\phi=1.5$. Strictly speaking, the formation and coalescence of antiphase domains can be studied only by examining the vacancy migration path for a large number of jumps. This is true because the larger, more stable domains were usually not built up independently of one another. Only small domains were formed independently. In addition, several vacancy path traverses along the boundary region between two nearly formed domains were usually required to minimize the boundary energy and thus stabilize the domains. This process terminated with the vacancy being ejected into a new, unexplored region. A striking feature of domain formation was the transitory appearance of small unstable domains which result from the emanation and retraction of spurs on the effective path.

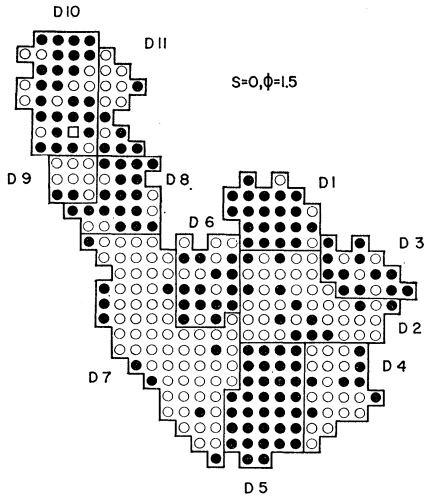

FIG. 9. Occupancy pattern of the 500-jump migration region at the completion of 500 jumps.

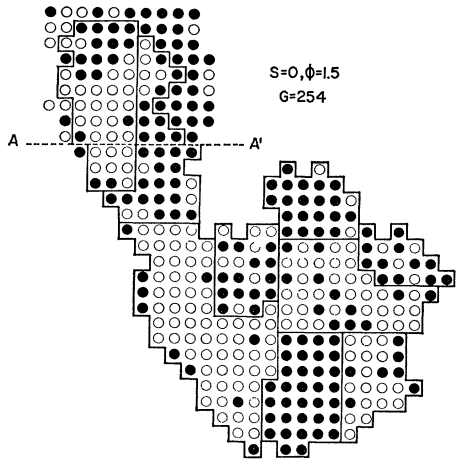

FIG. 10. The portion of Fig. 9 affected by vacancy migration after 500 jumps lies above the line AA'.

Three general characteristics were observed during domain formation: (1) Most of the configurational energy decrease due to local ordering was contributed when the effective path followed strings of minority sites. (2) The coalescence of antiphase domains tended to proceed with only a small decrease in the configurational energy. (3) Large domains were the result of several vacancy path traverses which entered the nascent domain region from different directions. The example given is a partial history of 500 jumps at the beginning of a 30 000 jump history. It was chosen because it illustrates each of the above points and at the same time is sufficiently short that one can describe it comprehensively in a relatively brief discussion.

Figure 8 describes the initial occupancy pattern of that part of the disordered crystal in which the 500-jump history took place. In this particular case the effective path was composed of 242 jumps, hence, about one-half of the total 500 jumps contributed nothing to either the ordering process or the transport of atoms and the vacancy. The outlines in Fig. 8 define eleven sectors. An antiphase domain occupied each of these

TABLE II. Occupancy and order changes during a 500-jump migration history for $S_i=0$ and $\phi=1.5$. N_R and N_W are the number of right and wrong sites, respectively. $S=(N_R-N_W)/(N_R+N_W)$.

Sector	Before N_R	Before N_W	After N_R	After N_W	Before S	After S	ΔN_R	$\Sigma(\Delta N_R)$
$R1$	15	8	20	3	0.309	0.74	+5	5
$W2$	20	24	12	32	−0.091	−0.455	−8	−3
$R3$	9	7	12	4	0.125	+0.50	+3	0
$W4$	11	13	7	17	−0.083	−0.417	−4	−4
$R5$	20	14	34	0	0.176	1.0	+14	10
$R6$	11	11	14	8	0	0.273	+3	13
$W7$	30	43	10	63	−0.178	−0.726	−20	−7
$R8$	11	11	17	5	0	0.545	+6	−1
$W9$	2	7	2	7	−0.556	−0.556	0	−1
$R10$	14	21	24	10	−0.20	0.500	+10	+9
$W11$	6	8	6	8	−0.143	−0.143	0	+9

sectors at the completion of 500 jumps as shown in Fig. 9. The open square in $D10$ of Fig. 8 denotes the position of the vacancy at the end of 500 jumps. The starting position was in $D1$ at the third site from the top in the second column from the left. Nearly all sectors which initially contained a majority of R sites (W sites) developed into antiphase domains wherein this majority was strengthened; domain $D10$ was an exception to this trend. Both $D6$ and $D8$ initially contained an equal number of R and W sites and both of them ended up with positive order. No change occurred in the order of $D9$ and $D11$. $D1$, $D5$, and $D7$ are highly ordered domains. The order of $D5$ was perfect. Table II summarizes the results of ordering in each sector.

The domain formation process was complex even though the computational model is a relatively simple one. There was a strong tendency for several domains

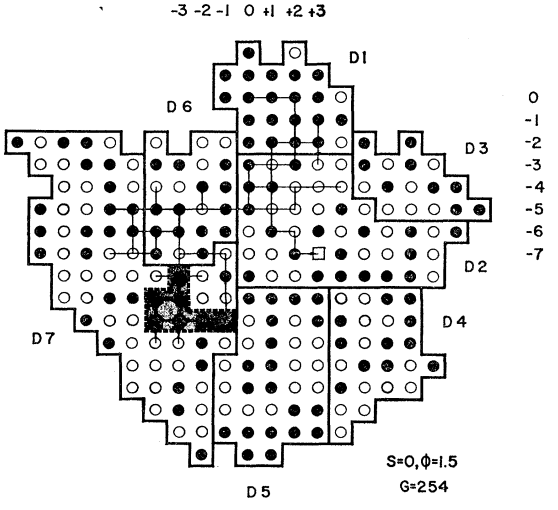

FIG. 11. Occupancy pattern after 100 jumps.

to be constructed concurrently and what appeared to be a well-formed nucleus would sometimes be assimilated by a less complete neighboring nucleus. Some domains, such as $D6$, served largely as passive corridors through which the vacancy shuttled back and forth, during the joint construction of larger, more perfect formations, without producing changes in the corridor domain itself.

Figure 10 is the occupancy pattern for the local region considered, after 30 000 jumps. $D8$ and $D9$ were extended upward into $D10$ and $D11$, respectively, by subsequent migration. The expansion of $D9$ illustrates the partial assimilation of an adjacent and larger domain by a small nucleus. The occupancy pattern below the line AA' was left unchanged. We will concern ourselves with those domains of the 500-jump migration region which were neither altered in occupancy nor extended during subsequent vacancy migration. These domains, $D1-D7$, were constructed in 407 jumps of

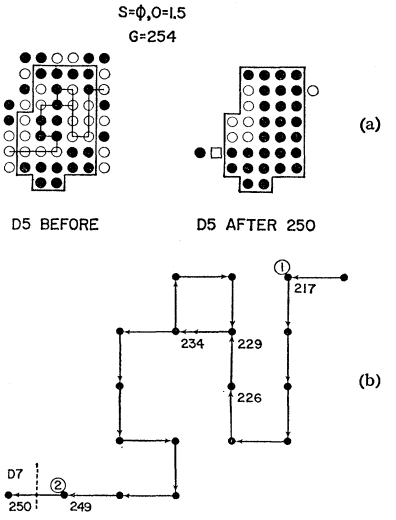

FIG. 12. Initial stage of the construction of antiphase domain $D5$.

which 207 were effective jumps. Their formation was accompanied by a configurational energy change of -85 units and the addition of seven W-sites.

Domains $D1-D7$ were constructed by vacancy migration centered about the point $(-1, -7)$ shown in Fig. 11. The course of events for the entire 407 jumps was largely determined by small scale ordering events occurring during the first 100 jumps (58 effective jumps). Figure 11 shows the occupancy pattern after 100 jumps and the associated migration path. In addition to the formation of $D1$ and $D6$, a small but important block, B, of seven W sites was formed in $D7$ as indicated by the dashed outline in Fig. 11. This block later served as the center of an order trap which was instrumental in determining the final occupancy of $D5$ and $D7$. The alternating $W-R-W-R-W$ configuration at the bottom of $D6$ was used as a route to circumvent B.

A comparison of Figs. 8 and 11 shows that $D1$ was formed as a consequence of the vacancy following a minority string of W sites. Three traverses entailing a total of 110 jumps (68 effective jumps) formed $D2$. $D3$ and $D4$ were created by single path traverses and

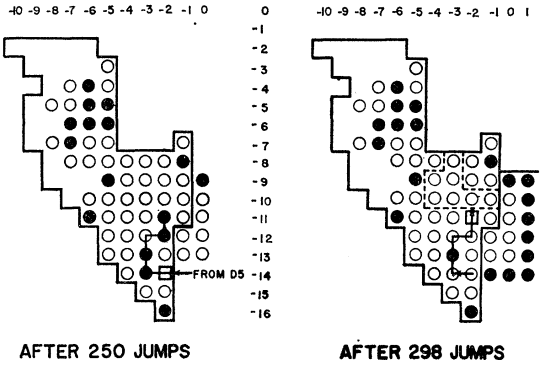

FIG. 13. Vacancy moving into an order trap along a minority string.

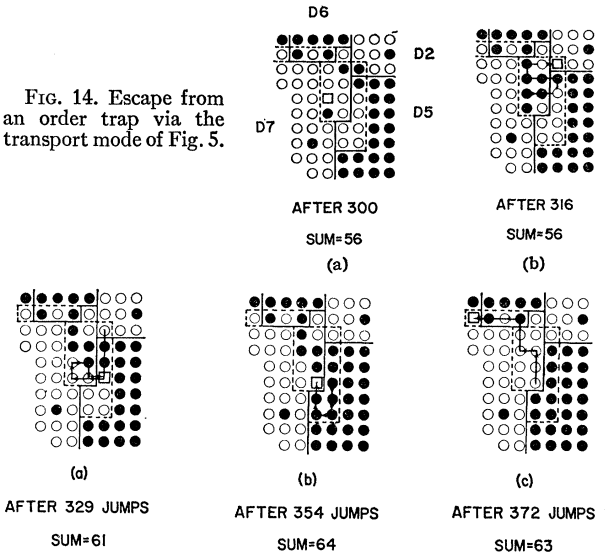

FIG. 14. Escape from an order trap via the transport mode of Fig. 5.

FIG. 15. Establishment of the boundary between domains $D5$ and $D7$.

$D3$ is an example of a domain formed without there being a change in configurational energy. A set of loops similar to those observed when isolated minority sites were removed from otherwise perfectly ordered systems were the basis for ordering in $D4$. The configurational energy change was -5 units.

By far the most interesting formation process was the joint construction of $D7$ and $D5$. The initial traverse through $D5$ is described by Fig. 12. It is composed of two strong segments and a 5-jump loop. The configurational energy change was -13 units, with -4 units contributed by the loop. Eleven W sites were converted to R sites leaving a block of six W sites yet to be converted if we view the formation process from the standpoint of the final position of the domain boundaries. The succeeding 23-jump traverse in $D7$ (jumps 250–273) contributed only five effective jumps and moved the vacancy along the string of R sites, indicated in Fig. 13, which terminates at the W-site block, B, established during the first 100 jumps. With the minority string removed, the vacancy found itself in a perfectly ordered region with one isolated minority site and the migration behavior reverted temporarily to that observed in perfectly ordered systems. Figures 14 and 15 show how the vacancy escaped from the order trap and illustrate what seems to be the principal mode for domain coalescence. The jump series 273–297 was made up of pairs of canceling jumps, characteristic of order trapping. Figure 14(a) describes the occupancy

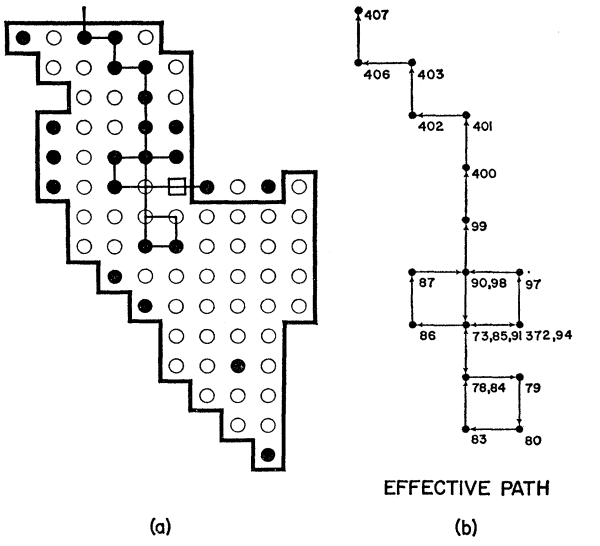

FIG. 16. Final stage in the construction of antiphase domain $D7$. (a) Occupancy pattern seen by the vacancy upon entering $D7$ from $D6$. (b) Effective path followed in removing R sites in (a) during jumps 372–407. (Numbers 73, 74, ···, 99 are to be read as 373, 374, ···, 399.)

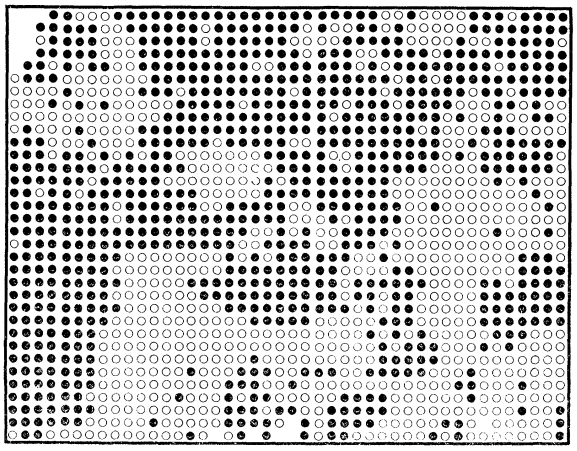

FIG. 17. Antiphase domain structure in a section of an occupancy map for 30 000 jumps for $S_i=0$ and $\phi=1.5$.

pattern and vacancy position after jump 300, the point at which the escape from the trap began. Trap escape was accomplished via the formation of a block of minority sites (R sites) which is consistent with the behavior observed in perfectly ordered systems. The details of the escape path are recorded in Fig. 14(b). After jump 316, the vacancy found itself both on the $D7$–$D5$ and $D2$–$D5$ boundaries. It chose to follow the $D7$–$D5$ boundary along the path defined by Fig. 15(a) establishing R sites in $D5$ and W sites in $D7$. This type of boundary traverse behavior is a typical feature of antiphase domain coalescence. Six changes in occupancy were effected with an energy change of -5 units, a little less than half the minimum energy change for the same occupancy change in a minority string path. The loop path set up an exit line of R sites leading into $R6$ which was later used to lead the vacancy out of the $D7$–$D5$ boundary region. $D5$ was completed at the termination of the jump sequence (329–354) of Fig. 15(b) which led into the exit line of R sites mentioned previously. An exit from the $D7$–$D5$ boundary stabili-

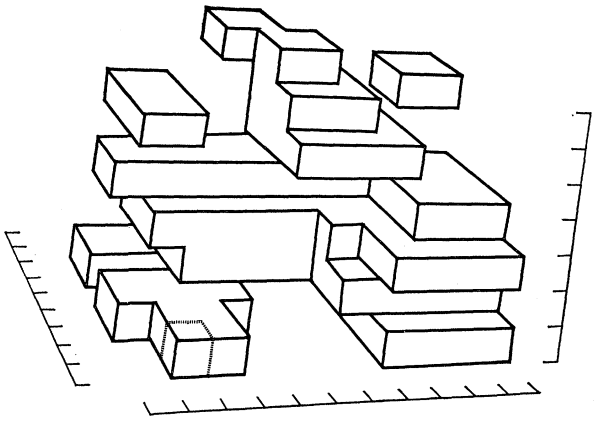

FIG. 18. Antiphase domain in the simple cubic lattice. An atomic volume is indicated in the lower left corner of the figure.

zation venture took place with no energy change along the path outlined in Fig. 15(c). The entire boundary stabilization jump sequence (300–372) changed the occupancy of 14 sites but produced an energy change of only -7 units. Figure 16 shows how the upper portion of $D7$ was completed in 21 effective jumps and an energy change of -22 units, about 25% of the total energy change of -85 units for the entire $D1$–$D7$ formation sequence.

Part of the occupancy map after 30 000 jumps is given in Fig. 17. This map shows that an expanding system of interlocking antiphase domains was constructed. The antiphase domain structure is strikingly similar to that observed by Marcinkowski and Brown[14] in systems which exhibit isotropically oriented antiphase boundaries. Because the energy change per effective jump in the domain coalescence process appears to be somewhat less than half that associated with the first stage of domain formation, the vacancy tends to move out into unexplored territory rather than re-enter the previously constructed migration region along domain boundaries. In this sense, the migration path has a tendency for self-avoidance. As a result of the self-avoidance tendency, domain coalescence is inhibited until the systems of contiguous antiphase domains developed by each individual vacancy come into contact and there is no mechanism for minimizing the free energy other than coalescence. This viewpoint is somewhat different than that suggested by Sykes and Jones[15] and Burns and Quimby[16] who considered coalescence to begin when individual, independently formed, ordered nuclei come into contact with each other. Although the work of tracing out domain formation in the bcc lattice is not yet complete, it appears as if a single vacancy also builds isolated ordered nuclei as well as contiguous antiphase domains in this lattice. Domain formation in the SCL is exemplified by the single domain shown in Fig. 18.

[14] M. J. Marcinkowski and N. Brown, J. Appl. Phys. **33**, 537 (1962).
[15] C. Sykes and F. W. Jones, Proc. Roy. Soc. (London) **A157**, 213 (1936); **A166**, 376 (1938).
[16] F. Burns and S. L. Quimby, Phys. Rev. **97**, 1567 (1955).

5. MIGRATION EXTENT

An estimate of how much the presence of an ordering energy affects the size of the vacancy migration region was obtained by comparing the size of the migration for $\phi>0$ with that for a symmetric random walk ($\phi=0$). This estimate has direct physical significance for $S_i=0$ and $S_i=1$. In these instances both the initial long-range and short-range order are sampled correctly. In all other instances the initial short-range order is too small because occupancy sampling was based solely on S_i. As a consequence, for $0<S<1$ the degree of contraction estimated is a lower limit for the true degree of contraction.

The number of sites, Σ_r, visited by the vacancy in a symmetric random walk of N jumps was found to be

$$\Sigma_{r2}(N)=0.714N^{0.90}, \quad \text{(SPL)} \tag{4a}$$

$$\Sigma_{r3}(N)=0.667N, \quad \text{(SCL)} \tag{4b}$$

$$\Sigma_{r3}(N)=0.72N, \quad \text{(bcc)} \tag{4c}$$

for the square planar lattice (SPL), simple cubic lattice (SCL), and body-centered lattice, respectively. For $\phi>0$ the number of sites visited was

$$\Sigma_2(S_i,\phi,N)=A(S_i,\phi)N^{x(S_i,\phi)}, \quad \text{(SPL)} \tag{5a}$$

$$\Sigma_3(S_i,\phi,N)=B(S_i,\phi)N, \quad \text{(SCL)}. \tag{5b}$$

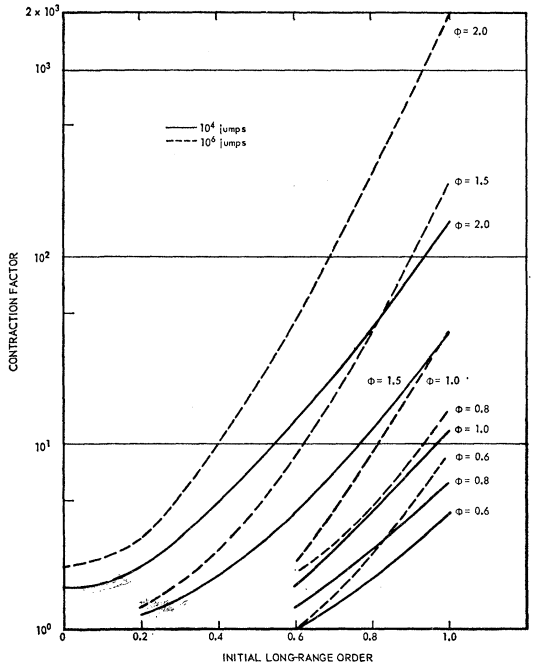

FIG. 19. Contraction factor for the square planar lattice.

TABLE III. Contraction factor (C_3) for the simple cubic lattice.

S	ϕ	Slope ($d\Sigma/dN$)	CF
0	0.405	0.676	0.99
0	0.6	0.690	0.97
0	0.8	0.703	0.95
0	1.0	0.715	0.93
0	1.2	0.726	0.92
0	1.4	0.736	0.91
1	0	0.667	1.00
1	0.405	0.204	3.27
1	0.6	0.074	9.01

The coefficient A in Eq. (5a) ranges from 0.6 to 1.0 with an average value of about 0.8. This magnitude is sufficiently close to the prefactor 0.714 in Eq. (4a) that the difference will be ignored in this discussion. The contraction factor $C(S_i,\phi)$ is defined as the ratio $\Sigma_r(N)/\Sigma(S_i,\phi,N)$ as in Eq. (6). It represents how much larger is the vacancy migration region for a symmetric random walk of N jumps than that for the same number of jumps in an orderable system. Because single vacancy migration proceeds as a symmetric random walk in a metal, the contraction factor, therefore, compares the migration extent for N jumps in a metal with that for N jumps in an orderable alloy having the same lattice structure as the metal. Let C_2 represent the contraction factor for the SPL and C_3 that for the SCL. C_2 is plotted in Fig. 19 for 10^4 and 10^6 jumps and C_3 is listed in Table III.

$$C_2=N^{(0.9-x)}, \quad \text{(SPL)} \tag{6a}$$

$$C_3=0.667/B, \quad \text{(SCL)}. \tag{6b}$$

These results pertain to that part of a vacancy migration history for which the migration regions of individual vacancies do not overlap. Hence, the range of applicability is a number of jumps, N, at least as large as the reciprocal of the vacancy concentration expressed in number of vacancies per lattice site.

The SCL contraction factor is considerably smaller than that for the SPL and is independent of the number of jumps. This suggests that an ordering energy inhibits surface diffusion and diffusion in thin films more than diffusion in bulk material. Computations for bcc and fcc lattices are in progress and will be reported in a subsequent paper.

6. COMPARISON WITH BETHE'S FIRST APPROXIMATION

A. Planar Lattice

Starting with $S_i=1(\sigma_i=1)$ ϕ was assigned the value 0.942 which, in Bethe's first approximation,[7,17] is associated with $S=0.9$ and $\sigma=0.845$ at equilibrium. Flinn and McManus[1] found that, in a fixed-volume, periodic approximation calculation for 2000 atoms, equilibrium LRO was established in 20 000 vacancy moves. In our expanding migration calculations the LRO and SRO of the set of sites visited by the vacancy oscillated about the values $S=0.87$ and $\sigma=0.84$, respectively, after about 15 000 jumps. Starting with $S_i=0$ ($\sigma_i=0$) and $\phi=\phi_c=0.693$, the LRO remained near zero (±0.02) and the SRO increased slowly to 0.32 at the end of 30 000 jumps. The equilibrium value given by Bethe for the critical temperature is 0.333. Starting with $S_i=0.5774$, to give $\sigma_i=S^2=0.333$ and again using $\phi=0.693$, the SRO leveled off 0.379 and LRO at 0.14 for 15 000 jumps. The existence of $S>0$ at the boundary of the migration region precludes convergence of S to the equilibrium value inside an *isolated* expanding migration region.

B. Simple Cubic Lattice

Starting with $S_i=\sigma_i=0$ and $\phi=\phi_c=0.405$, the SRO increased to 0.235 at 10 000 jumps and the LRO remained at zero. Bethe's model gives $\sigma=0.2$ and $S=0$ for $\phi=0.405$. With $\phi=0.6$, the SCL disordered from $S_i=\sigma_i=1$ to $S=0.93$ and $\sigma=0.87$ in 10 000 jumps. The migration region was sufficiently small ($\sim$2300 sites) that all runs could be extended to 30 000 jumps in this instance. The order attained at 10 000 jumps was retained up to the end of the 30 000 jump histories. Bethe's first approximation gives $S=0.91$ and $\sigma=0.845$ for $\phi=0.6$. The slightly larger values obtained in the Monte Carlo experiments are ascribed in the boundary effect mentioned above.

[17] H. Bethe, Proc. Roy. Soc. (London) **A150**, 552 (1935).

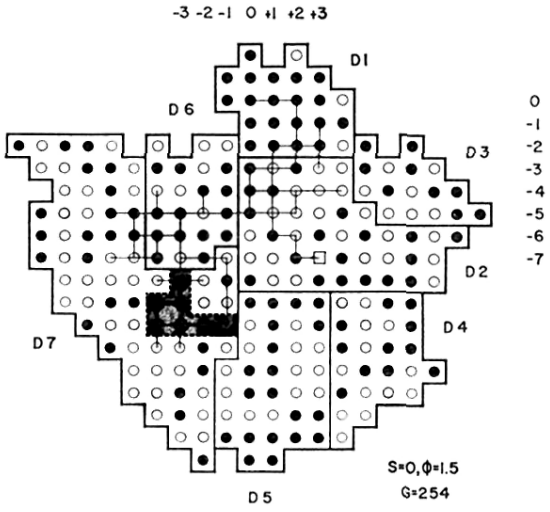

FIG. 11. Occupancy pattern after 100 jumps.